Toward a Microscopic Description of Nucleus-Nucleus Collisions

Matteo Vorabbi,[1] Michael Gennari,[2,3] Paolo Finelli,[4] Carlotta Giusti,[5] and Petr Navrátil[2,3]
[1]School of Mathematics and Physics, University of Surrey, Guildford, GU2 7XH, United Kingdom
[2]TRIUMF, 4004 Wesbrook Mall, Vancouver, British Columbia, V6T 2A3, Canada
[3]University of Victoria, 3800 Finnerty Road, Victoria, British Columbia V8P 5C2, Canada
[4]Dipartimento di Fisica e Astronomia, Università degli Studi di Bologna and INFN, Sezione di Bologna, Via Irnerio 46, I-40126 Bologna, Italy
[5]INFN, Sezione di Pavia, Via A. Bassi 6, I-27100 Pavia, Italy

(Received 15 October 2024; revised 30 April 2025; accepted 18 September 2025; published 21 October 2025)

We present the first results of a comprehensive microscopic approach to describe nucleus-nucleus elastic collisions by means of an optical potential derived at first order in multiple-scattering theory and computed by folding the projectile and target nuclear densities with the nucleon-nucleon t matrix, which describes the interaction between each nucleon of the projectile and each nucleon of the target. Chiral interactions are consistently used in the calculation of the t matrix and of the nonlocal nuclear densities, which are computed within the *ab initio* no-core shell model. Cross sections calculated for α collisions on ^{12}C and ^{16}O at projectile energies in the range 100–300 MeV are presented and compared with available data. For momentum transfer q up to about 1.0 fm^{-1} our results are in good agreement with the experimental data, whereas for higher momenta a reduction of the imaginary contributions is needed.

DOI: 10.1103/qxtf-5b4y

Nucleus-nucleus collisions are fundamental processes that provide insight into the properties of nuclear matter and the dynamics of heavy-ion interactions. They are usually described by traditional phenomenological models which often rely on tunable parameters to fit experimental data, limiting their predictive power, particularly concerning exotic nuclei. The study of microscopic optical potentials (OPs) has been and still is a fascinating area of research in nuclear physics, since they play a crucial role in understanding the interactions of nucleons in atomic nuclei [1–4] and in describing nucleon-nucleus and nucleus-nucleus interactions. From the experimental point of view, in the past decade a large effort has been made to study short-lived exotic nuclei using proton elastic scattering in inverse kinematics at facilities such as the CSRe storage ring of HIRFL-CSR [5], GSI/FAIR [6], and the RIBF at RIKEN [7]. In the near future the dynamics of elastic scattering involving light bound nuclei will likely receive considerable attention as a probe of unexpected deviations from the theoretical expectations based on our present knowledge of the nucleon-nucleon interaction.

In general, OPs have broad implications across various nuclear reactions, such as nucleon-induced reactions or fusion processes. OPs find applications in astrophysics, where they are crucial for modelling nucleosynthesis in stars and understanding stellar evolution [8], but they also play a significant role in nuclear energy applications, such as reactor design and fuel cycle simulations [9].

The importance of a microscopic description of nucleus-nucleus collisions is also connected to the relevance for hadron-therapy applications and space radiation protection [10]. In fact, modeling the space radiation environment is a crucial step in planning for space missions and the analysis of shielding efficiency. The space radiation transport codes used to describe the transport of ions and secondary particles produced from nuclear collisions require knowledge of the relevant nuclear reactions, among them elastic scattering. At the moment such reactions are described by phenomenological models [11,12] due to theoretical limitations and the scarcity of data.

Since microscopic approaches are derived from first principles, they ensure consistency with the underlying physics. These methods incorporate fundamental interactions, nuclear structure information, and experimental constraints to construct a comprehensive picture of nuclear systems. As a result, microscopic approaches provide a more fundamental understanding of the phenomena and avoid ad hoc assumptions usually included in phenomenological descriptions. Microscopic models offer the advantage of an enhanced predictive power, allowing them to rigorously extrapolate beyond the experimental data used to construct the OP. This predictive capability is crucial for investigating unexplored regions of the nuclear chart, exotic nuclei, and nuclear reactions under extreme conditions, e.g., those encountered in astrophysical environments. By employing solid theoretical models it is possible to make significant progress in the interpretation of the complex nature of these potentials and their impact on nuclear phenomena [4].

In this Letter we present a model to derive a microscopic nucleus-nucleus OP from the multiple-scattering theory.

We refer to Supplemental Material [13] for a sketch of the main steps of the derivation of the OP, as well as for some computational and numerical details. At first order in the theory, corresponding to the single-scattering approximation, the OP for elastic nucleus-nucleus collisions is obtained from the double-folding integral of the free nucleon-nucleon (NN) t matrix and the densities of the projectile ($\mathbb{P}$) and target ($\mathbb{T}$) nuclei, $\rho^{(\mathbb{P})}$ and $\rho^{(\mathbb{T})}$, respectively. In our approach, the NN t matrix plays the role of an effective interaction between a proton or neutron (p or n) in $\mathbb{P}$ and a proton or neutron in $\mathbb{T}$. The general formula of our OP is then given by [13]

$$U_{\rm el}(\boldsymbol{q},\boldsymbol{K};E) = \sum_{\alpha,\beta=p,n}\int d\boldsymbol{Q}_{\mathbb{P}}\int d\boldsymbol{Q}_{\mathbb{T}}\eta(\boldsymbol{q},\boldsymbol{K},\boldsymbol{Q}_{\mathbb{P}},\boldsymbol{Q}_{\mathbb{T}})t_{\alpha\beta}\left[\boldsymbol{q},\frac{1}{2}\left(\frac{A_{\mathbb{P}}+A_{\mathbb{T}}}{A_{\mathbb{P}}A_{\mathbb{T}}}\boldsymbol{K}-\sqrt{\frac{A_{\mathbb{P}}-1}{A_{\mathbb{P}}}}\boldsymbol{Q}_{\mathbb{P}}+\sqrt{\frac{A_{\mathbb{T}}-1}{A_{\mathbb{T}}}}\boldsymbol{Q}_{\mathbb{T}}\right);\mathcal{E}\right]$$
$$\times\rho_{\alpha}^{(\mathbb{P})}\left(\boldsymbol{Q}_{\mathbb{P}}-\frac{1}{2}\sqrt{\frac{A_{\mathbb{P}}-1}{A_{\mathbb{P}}}}\boldsymbol{q},\boldsymbol{Q}_{\mathbb{P}}+\frac{1}{2}\sqrt{\frac{A_{\mathbb{P}}-1}{A_{\mathbb{P}}}}\boldsymbol{q}\right)\times\rho_{\beta}^{(\mathbb{T})}\left(\boldsymbol{Q}_{\mathbb{T}}+\frac{1}{2}\sqrt{\frac{A_{\mathbb{T}}-1}{A_{\mathbb{T}}}}\boldsymbol{q},\boldsymbol{Q}_{\mathbb{T}}-\frac{1}{2}\sqrt{\frac{A_{\mathbb{T}}-1}{A_{\mathbb{T}}}}\boldsymbol{q}\right). \quad (1)$$

In Eq. (1) the variables $\boldsymbol{q}=\boldsymbol{k}'-\boldsymbol{k}$ and $2\boldsymbol{K}=\boldsymbol{k}'+\boldsymbol{k}$ are the momentum transfer and the average momentum, respectively, where $\boldsymbol{k}$ and $\boldsymbol{k}'$ are the initial and final relative momenta in the nucleus-nucleus frame; $\boldsymbol{Q}_{\mathbb{P}}$ and $\boldsymbol{Q}_{\mathbb{T}}$ are integration variables, $A_{\mathbb{P}}$ and $A_{\mathbb{T}}$ the number of nucleons of the projectile and of the target and η the Møller factor that imposes the Lorentz invariance between different reference systems, as discussed in Supplemental Material [13].

The energy $\mathcal{E}$ at which the NN t matrix is computed is a complicated function of $\boldsymbol{K}$, $\boldsymbol{Q}_{\mathbb{P}}$, and $\boldsymbol{Q}_{\mathbb{T}}$, and makes the calculation of Eq. (1) unfeasible. In the present work this is set to one-half the kinetic energy of a single nucleon in the projectile nucleus (see Ref. [13] for more details).

We note that the t matrix entering Eq. (1) only contains the central (spin-independent) term, because the other terms lead to small or vanishing contributions. Consequently, our OP only contains the central term. However, we would like to stress that this term contains both real (V) and imaginary (W) parts, such that $U=V+iW$. In particular, the imaginary part is produced in the calculation by the imaginary part of the t matrix.

The use of the free two-nucleon scattering operator is an approximation that reduces the complexity of the original many-body problem to a form in which we only have to solve two-body equations, neglecting the effect of nuclear binding on the two interacting nucleons.

In this Letter we present numerical results of the cross sections obtained with the microscopic OP of Eq. (1) for a selected set of cases of ^{4}He elastic scattering off ^{12}C and ^{16}O at three incoming energies, 104, 130, and 240 MeV, for which experimental data are available.

For the calculation of the nonlocal density of the projectile and target nuclei in momentum space we employ the no-core shell model (NCSM) approach [33,34]. The NCSM is based on an expansion of the nuclear wave function in a harmonic oscillator basis characterized by the frequency $\hbar\omega$ and the basis truncation parameter N_{max}, which specifies the number of nucleon excitations above the lowest energy configuration allowed by the Pauli principle.

All our calculations have been performed with the NN chiral interaction developed by Entem *et al.* [35] up to the fifth order (N^{4}LO) with a 500 MeV cutoff and the three-nucleon ($3N$) local-nonlocal chiral interaction at N^{2}LO presented in Refs. [36,37], with the low-energy constants fixed at $c_D=-1.8$ and $c_E=-0.31$ [38]. The same NN chiral interaction used to compute the nuclear densities is consistently used in the calculation of the NN t matrix. For the three nuclei we employed $\hbar\omega=18$ MeV and a $\lambda_{\rm SRG}=1.8$ fm^{-1} cutoff for the similarity renormalization group (SRG) [39,40] procedure (including the SRG induced 3N force in all the calculations), and we performed calculations up to $N_{max}=8$ for ^{12}C and ^{16}O, and $N_{max}=16$ for ^{4}He.

In Figs. 1 and 2 we display in solid red lines the differential cross sections (divided by the Rutherford cross section) obtained with our OP as a function of the momentum transfer q for the ^{12}C(^{4}He, ^{4}He)^{12}C and ^{16}O(^{4}He, ^{4}He)^{16}O reactions, respectively, at the three aforementioned energies. In both figures our OP gives a good description (size, shape, position of the minima) of the experimental data for values of $q\leq 1.0$ fm^{-1}, showing that our microscopic model, which does not contain adjustable parameters, is theoretically well founded and should have good predictive power in situations for which empirical data are not yet available, e.g., for exotic nuclei. In both figures, however, for larger values of q our results underpredict the data and the disagreement increases with q. The reason for the disagreement is not clear, but it is likely due to the approximate description of the interaction of a nucleon in the projectile and a nucleon in the target by the free NN t matrix, which seems to introduce an excessive contribution from the absorptive imaginary part of the OP in the model. In order to test this hypothesis, we performed calculations with an artificially reduced imaginary component multiplied by 0.5. This reduction (the corresponding results are depicted by red dashed lines in

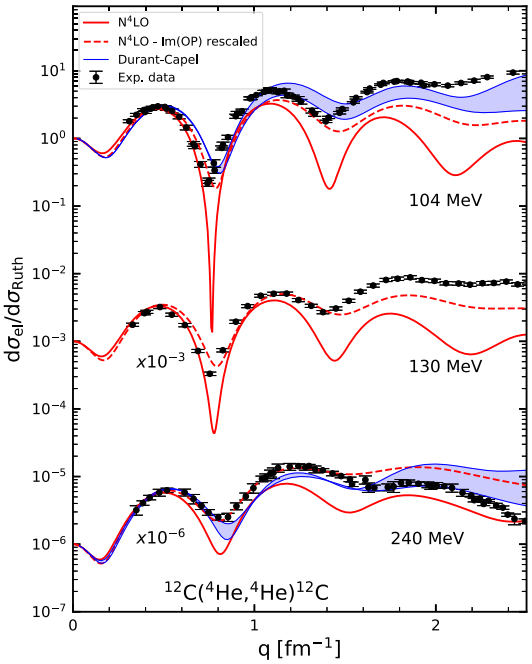

FIG. 1. Ratio of the differential cross section to the Rutherford cross section as a function of the transferred momentum q for the reaction ^{12}C(^{4}He, ^{4}He)^{12}C. Calculations are performed at projectile energies $E = 104$, 130, and 240 MeV. Experimental data [41–43] are shown by black circles with corresponding error bars. The solid red lines are obtained using our microscopic OP of Eq. (1); red dashed lines are obtained rescaling the imaginary part of our OP by a factor 0.5. The results obtained in Ref. [44] are shown by the shaded blue bands for a comparison.

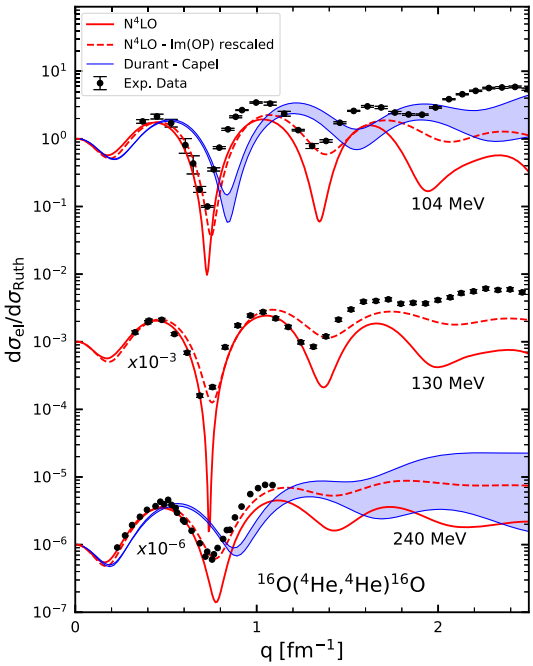

FIG. 2. The same as in Fig. 1 but for the reaction ^{16}O(^{4}He, ^{4}He)^{16}O.

the figures) barely changes the behaviour at small q, whereas it substantially improves the agreement up to large values of the momentum transfer.

As a benchmark, recent calculations by Durant and Capel [44] are also shown in the figures by the light blue bands. In Ref. [44] the OP is obtained from the double-folding method using chiral NN interactions at N^{2}LO [45] and realistic nuclear densities; the bands give theoretical uncertainties by use of different cutoff radii in the chiral interaction and different nuclear densities. A few years ago we performed a similar investigation for proton-nucleus elastic scattering, showing that a satisfactory level of convergence could be achieved once chiral interactions developed up to N^{4}LO are employed [46]. For the nucleus-nucleus case, the sensitivity of our theoretical predictions upon different interactions and truncation schemes has been studied in Supplemental Material [13], as shown in Figs. S1 and S2.

In Ref. [44] the imaginary part of the OP is obtained from the real one, either, as in phenomenological approaches [47,48], multiplying the real part by a proportionality constant

$$W = N_W V, \tag{2}$$

with N_W in the range 0.5-0.8, or linking the two parts by applying the Kramers-Kronig dispersion relations

$$W(E) = -\frac{1}{\pi}\mathcal{P}\int_{-\infty}^{\infty}\frac{V_{\mathrm{Ex}}(E')}{E'-E}dE', \tag{3}$$

where $\mathcal{P}$ denotes the Cauchy principal value of the integral and V_{Ex} the exchange part of the real component. Eq. (3) ensures that the OP is constrained by the correct energy dependence of the imaginary absorptive part. In Ref. [44] the two prescriptions give similar results, even if the Kramers-Kronig relations yield better agreement with data, for large values of q and without any free parameter. The light blue bands in Figs. 1 and 2 are computed with the imaginary part obtained with Eq. (3). In any case both prescriptions give results closer to our dashed line than to our solid lines, i.e., to our results with the reduced imaginary part of our OP.

Additional information concerning the connection between the phenomenological and the microscopic description of the absorptive component of the optical potential can be obtained by looking separately at the real and imaginary parts. As mentioned previously, in phenomenological approaches a typical prescription is given by Eq. (2). This choice is based on the underlying assumption that W and V have a similar behavior as functions of the relevant coordinates. In Fig. 3 we show with the dashed blue lines the results obtained adopting Eq. (2), where the imaginary part of our microscopic OP is replaced by the real part multiplied by 0.5. We can see that for all three

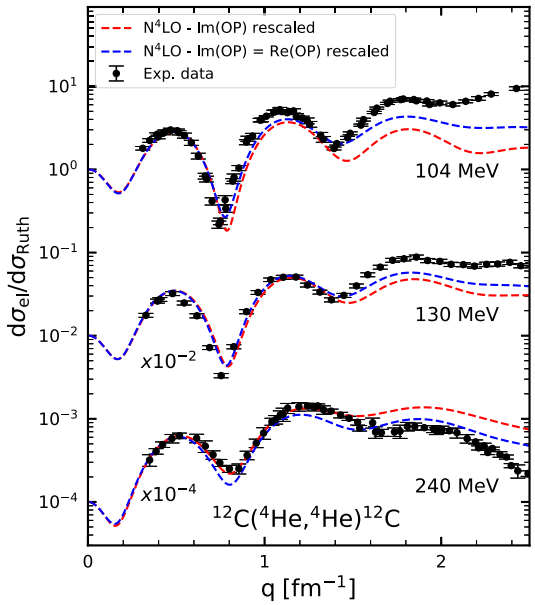

FIG. 3. Ratio of the differential cross section to the Rutherford cross section as a function of the transferred momentum q for the reaction ^{12}C(^{4}He, ^{4}He)^{12}C. The dashed red lines are the same as in Fig. 1; the dashed blue lines are the corresponding results obtained replacing the imaginary part of our OP with its real part rescaled by the same factor 0.5.

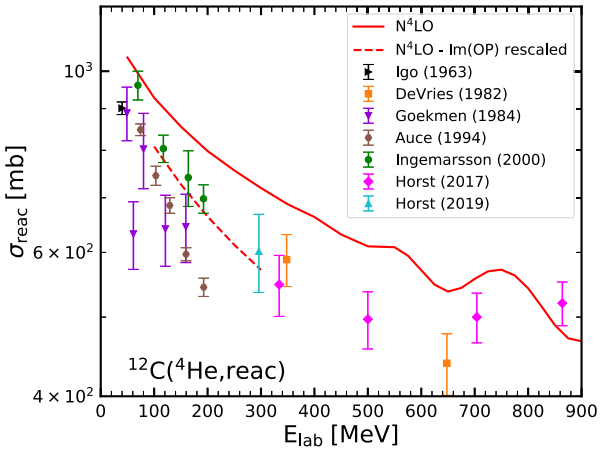

FIG. 4. Reaction cross section ^{12}C (^{4}He, reac) as a function of the projectile laboratory energy E_{lab}. The solid red line is the result of our microscopic OP; the dashed red line is obtained rescaling the imaginary part of our OP by a factor 0.5. Experimental data are shown by filled colored symbols with the corresponding error bars: rightward black triangles [49], orange squares [50], downward violet triangles [56], brown circles [51–53], green circles [54], and pink diamonds [55].

energies the results obtained with the phenomenological prescription are very close to those obtained by rescaling the imaginary part (dashed red lines). In our analysis we have plotted the real and imaginary parts and have confirmed that they have very similar shapes. The reason why the two curves are not exactly the same is because the real and imaginary parts of the OP have slightly different depths and in this work we always rescaled the two parts with the same factor.

In Fig. 4 we show the reaction cross section ^{12}C (^{4}He, reac) in comparison with experimental data [49–55] that cover a large energy range (10–1100 MeV). Our results overestimate data but are able to describe their overall behavior, which is not trivial since microscopic approaches are usually able to reproduce angular distributions but not necessarily integrated quantities. Once the imaginary part has been halved, in the energy range 100–300 MeV (in which we are more confident about the approximations of our model and where the available differential cross section data allow the rescaling procedure), our results displayed by the dashed red line fall close to the experimental data.

In conclusion, we have presented the first results of a microscopic approach to describe nucleus-nucleus collisions. Our microscopic OP provides a good description of the experimental data for values of momentum transfer up to 1.0 fm^{-1} and underestimates the data for larger values. The disagreement between theoretical and experimental results in this region indicates that the OP seems to be too absorptive and a simple reduction of the imaginary part seems to confirm that.

The theoretical reason for this excess of absorption is however not clear. The model contains several approximations which might explain the disagreement with the data, such as the use of the free NN t matrix to describe the interaction between a nucleon in the projectile and one in the target, the prescription used to fix the energy $\mathcal{E}$ at which the t matrix is computed, or the single-scattering approximation adopted to derive the OP. Including multiple scattering effects can play a significant role, as discussed in Ref. [57] for the nucleon-nucleus case. The inclusion of medium effects [58] could be also helpful to reduce the disagreement with experimental data.

In spite of all the adopted approximations and without any free parameters our results are able to describe the overall behavior of the reaction cross section, which is not trivial, and are in remarkable agreement with the experimental differential cross section for values of $q \leq 1.0$ fm^{-1}. In our opinion, this is a clear indication that these first results represent a significant step towards a microscopic description and a more fundamental understanding of nuclear collisions.

Despite the overall quality of the description of experimental observables, our approach is well suited for improvements. Our theoretical model, we believe, can be improved through two main aspects: on the one hand, by analyzing and studying the various prescriptions for the energy variable of the propagator; on the other hand, by conducting a thorough investigation of the imaginary component of the optical potential, particularly exploring

the potential existence of a connection with the dispersive relations approach.

Our results highlight the significance of incorporating quantum mechanical effects (through sophisticated many-body methods like multiple-scattering theory) and detailed nuclear descriptions of projectiles and targets (by *ab initio* methods like the NCSM approach) to accurately describe the optical potential. These findings not only provide deeper insights into the fundamental processes governing nuclear interactions but also pave the way for more accurate and predictive models in nuclear physics, particularly for exotic nuclei. Future work should aim to refine these models further and explore their implications for a broader range of nuclear phenomena.

Acknowledgments—We would like to thank P. Capel and V. Durant (University of Mainz) for useful discussions and providing results presented in Ref. [44]. This work used the DiRAC Data Intensive service (DIaL3) at the University of Leicester, managed by the University of Leicester Research Computing Service on behalf of the STFC DiRAC HPC Facility. The DiRAC service at Leicester was funded by BEIS, UKRI and STFC capital funding and STFC operations grants. DiRAC is part of the UKRI Digital Research Infrastructure. This work used the DiRAC Complexity system, operated by the University of Leicester IT Services, which forms part of the STFC DiRAC HPC Facility. This equipment is funded by BIS National E-Infrastructure Capital Grant No. ST/K000373/1 and STFC DiRAC Operations Grant No. ST/K0003259/1. DiRAC is part of the National e-Infrastructure. M. G. and P. N. acknowledge support from the NSERC Grant No. SAPIN-2022-00019. TRIUMF receives federal funding via a contribution agreement with the National Research Council of Canada. Computing support also came from an INCITE Award on the Summit and Frontier supercomputers of the Oak Ridge Leadership Computing Facility (OLCF) at ORNL and from the Digital Research Alliance of Canada.

M. V. and P. F. contributed equally to this work.

[1] L. Foldy and J. Walecka, Ann. Phys. (Berlin) **54**, 447 (1969).
[2] P. E. Hodgson, Rep. Prog. Phys. **34**, 765 (1971).
[3] W. Dickhoff and R. Charity, Prog. Part. Nucl. Phys. **105**, 252 (2019).
[4] C. Hebborn *et al.*, J. Phys. G **50**, 060501 (2023).
[5] J. W. Xia *et al.*, Nucl. Instrum. Methods Phys. Res., Sect. A **488**, 11 (2002).
[6] N. Kalantar-Nayestanaki and A. Bruce, Nucl. Phys. News **28**, 5 (2018).
[7] H. Sakurai, in *Perspective in Nuclear Physics*, American Institute of Physics Conference Series Vol. 1120, edited by S.-C. Jeong, Y. Utsuno, T. Motobayashi, and A. Bracco (AIP, 2009), pp. 241–246.
[8] P. Descouvemont, Front. Astron. Space Sci. **7**, 9 (2020).
[9] L. A. Bernstein, D. A. Brown, A. J. Koning, B. T. Rearden, C. E. Romano, A. A. Sonzogni, A. S. Voyles, and W. Younes, Annu. Rev. Nucl. Part. Sci. **69**, 109 (2019).
[10] J. M. Figueira, J. O. F. Niello, A. Arazi, O. A. Capurro, P. Carnelli, L. Fimiani, G. V. Martí, D. M. Heimann, A. E. Negri, A. J. Pacheco, J. Lubian, D. S. Monteiro, and P. R. S. Gomes, Phys. Rev. C **81**, 024613 (2010).
[11] C. Ahdida *et al.*, Front. Phys. **9**, 788253 (2022).
[12] R. E. Azuma, E. Uberseder, E. C. Simpson, C. R. Brune, H. Costantini, R. J. de Boer, J. Görres, M. Heil, P. J. LeBlanc, C. Ugalde, and M. Wiescher, Phys. Rev. C **81**, 045805 (2010).
[13] See Supplemental Material at http://link.aps.org/supplemental/10.1103/qxtf-5b4y for details about the derivation of the optical potential, which includes Refs. [14–41].
[14] K. M. Watson, Phys. Rev. **105**, 1388 (1957).
[15] G. Satchler and W. Love, Phys. Rep. **55**, 183 (1979).
[16] F. A. Cucinotta, Theory of alpha-nucleus collisions at high energies, Ph.D. thesis, Old Dominion University, 1988.
[17] J. M. Greben and S. A. Gurvitz, Phys. Rev. C **36**, 1839 (1987).
[18] C. M. Werneth, K. M. Maung, W. P. Ford, J. W. Norbury, and M. D. Vera, Phys. Rev. C **90**, 064905 (2014).
[19] C. M. Werneth, W. P. Ford, J. W. Norbury, and M. D. Vera, Report No. NASA/TP-2014-218529, 2014.
[20] A. Picklesimer, Phys. Rev. C **24**, 1400 (1981).
[21] N. Austern, *Direct Nuclear Reaction Theories*, Interscience Monographs and Texts in Physics and Astronomy (Wiley-Interscience, New York, 1970).
[22] G. Satchler, *Direct Nuclear Reactions*, International Series of Monographs on Physics (Clarendon Press, Oxford, 1983).
[23] H. Feshbach, *Theoretical Nuclear Physics: Nuclear Reactions*, Theoretical Nuclear Physics Vol. 2 (Wiley, New York, 1992).
[24] M. Vorabbi, M. Gennari, P. Finelli, C. Giusti, P. Navrátil, and R. Machleidt, Phys. Rev. C **103**, 024604 (2021).
[25] C. R. Chinn, C. Elster, R. M. Thaler, and S. P. Weppner, Phys. Rev. C **52**, 1992 (1995).
[26] S. P. Weppner, C. Elster, and D. Hüber, Phys. Rev. C **57**, 1378 (1998).
[27] K. Kravvaris, K. R. Quinlan, S. Quaglioni, K. A. Wendt, and P. Navrátil, Phys. Rev. C **102**, 024616 (2020).
[28] L. Girlanda, A. Kievsky, and M. Viviani, Phys. Rev. C **84**, 014001 (2011); **102**, 019903(E) (2020).
[29] K. Kravvaris, P. Navrátil, S. Quaglioni, C. Hebborn, and G. Hupin, Phys. Lett. B **845**, 138156 (2023).
[30] L. Jokiniemi, P. Navrátil, J. Kotila, and K. Kravvaris, Phys. Rev. C **109**, 065501 (2024).
[31] S. Weppner, Microscopic calculations of first-order optical potentials for nucleon-nucleus scattering, Ph.D. thesis, Ohio University, 1997.
[32] C. J. Joachain, *Quantum Collision Theory* (North-Holland Publishing Company, Amsterdam, 1975).
[33] P. Navratil, S. Quaglioni, I. Stetcu, and B. R. Barrett, J. Phys. G **36**, 083101 (2009).
[34] B. R. Barrett, P. Navratil, and J. P. Vary, Prog. Part. Nucl. Phys. **69**, 131 (2013).
[35] D. R. Entem, R. Machleidt, and Y. Nosyk, Phys. Rev. C **96**, 024004 (2017).

[36] P. Navratil, Few Body Syst. **41**, 117 (2007).
[37] V. Somà, P. Navrátil, F. Raimondi, C. Barbieri, and T. Duguet, Phys. Rev. C **101**, 014318 (2020).
[38] P. Gysbers, G. Hagen, J. D. Holt, G. R. Jansen, T. D. Morris, P. Navrátil, T. Papenbrock, S. Quaglioni, A. Schwenk, S. R. Stroberg, and K. A. Wendt, Nat. Phys. **15**, 428 (2019).
[39] S. K. Bogner, T. T. S. Kuo, and A. Schwenk, Phys. Rep. **386**, 1 (2003).
[40] S. K. Bogner, R. J. Furnstahl, and A. Schwenk, Prog. Part. Nucl. Phys. **65**, 94 (2010).
[41] S. Adachi *et al.*, Phys. Rev. C **97**, 014601 (2018).
[42] G. Hauser, R. Löhken, H. Rebel, G. Schatz, G. Schweimer, and J. Specht, Nucl. Phys. **A128**, 81 (1969).
[43] B. John, Y. Tokimoto, Y.-W. Lui, H. L. Clark, X. Chen, and D. H. Youngblood, Phys. Rev. C **68**, 014305 (2003).
[44] V. Durant and P. Capel, Phys. Rev. C **105**, 014606 (2022).
[45] V. Durant, P. Capel, L. Huth, A. Balantekin, and A. Schwenk, Phys. Lett. B **782**, 668 (2018).
[46] M. Vorabbi, P. Finelli, and C. Giusti, Phys. Rev. C **96**, 044001 (2017).
[47] M. Alvarez, L. Chamon, M. Hussein, D. Pereira, L. Gasques, E. Rossi, and C. Silva, Nucl. Phys. **A723**, 93 (2003).
[48] D. Pereira, J. Lubian, J. Oliveira, D. de Sousa, and L. Chamon, Phys. Lett. B **670**, 330 (2009).
[49] B. D. Wilkins and G. Igo, Phys. Rev. **129**, 2198 (1963).
[50] R. M. DeVries, N. J. DiGiacomo, J. S. Kapustinsky, J.-C. Peng, W. E. Sondheim, J. W. Sunier, J. G. Cramer, R. E. Loveman, C. R. Gruhn, and H. H. Wieman, Phys. Rev. C **26**, 301 (1982).
[51] H. Abele, U. Atzrott, A. Auce, C. Hillenmayer, A. Ingemarsson, and G. Staudt, Phys. Rev. C **50**, R10 (1994).
[52] A. Ingemarsson, A. Auce, and R. Johansson, Phys. Rev. C **49**, 1609 (1994).
[53] A. Auce, R. F. Carlson, A. J. Cox, A. Ingemarsson, R. Johansson, P. U. Renberg, O. Sundberg, G. Tibell, and R. Zorro, Phys. Rev. C **50**, 871 (1994).
[54] A. Ingemarsson *et al.*, Nucl. Phys. **A676**, 3 (2000).
[55] F. Horst, C. Schuy, U. Weber, K.-T. Brinkmann, and K. Zink, Phys. Rev. C **96**, 024624 (2017).
[56] A. Gökmen, M. Dworzecka, and J. J. Griffin, Nucl. Phys. **A440**, 586 (1985).
[57] R. Crespo, R. C. Johnson, and J. A. Tostevin, Phys. Rev. C **46**, 279 (1992).
[58] H. F. Arellano, F. A. Brieva, and W. G. Love, Phys. Rev. C **52**, 301 (1995).